jnm/DIAGNOSTIC NUCLEAR MEDICINE

Tomographic Scintigraphy of Regional Myocardial Perfusion

B. Leonard Holman, John D. Idoine, Thomas A. Sos,* Roger Tancrell, and Gordon DeMeester

Harvard Medical School and Peter Bent Brigham Hospital, Boston, Massachusetts and Raytheon Company, Waltham, Massachusetts

Estimation of the extent of regional ischemia by scintigraphic methods has been hampered by the geometric constraints of two-dimensional imaging. Myocardial perfusion scintigraphy was performed using the Fresnel zone-plate tomographic camera after the injection of Tc-99m microspheres (20–40 μ) into a coronary artery. Coronary artery occlusion was performed in six dogs by embolization via a catheter guidewire system. Twenty millicuries of Tc-99m microspheres were injected into the left main coronary artery of the six occluded and three unoccluded dogs. Scintigraphy was performed in multiple projections in the living animal. Optical reconstruction of the holographic image provided tomographic gamma images of the heart. Scintigraphy was also performed with an Anger camera for comparison. The extent of the perfusion defect was measured by planimetry and expressed as a percentage of the ventricular area in that projection. The average of the right and left anterior oblique projections provided the most accurate estimate of the size of the perfusion defect (average error: 13.6%; range: 0–38.2%). Fresnel zone-plate imaging provided an accurate in vivo assessment of the extent of altered myocardial perfusion.

J Nucl Med 18: 764–769, 1977

Images of regional myocardial perfusion can be obtained after the intravenous injection of potassium analogues (*1–5*) or the coronary artery injection of radiolabeled particles (*6,7*). Attempts to estimate the size of the perfusion defect using gamma-emitting tracers have been hampered by the constraints of the resulting two-dimensional image.

Experimentally we have induced coronary ischemia and have injected microspheres tagged with technetium-99m into the left coronary artery. We then imaged the heart with a tomographic Fresnel zone-plate camera (*8*) to assess its effectiveness in locating and measuring the size of the ischemic region.

METHODS

Figure 1 is a photograph of the camera assembly. In this system, gamma photons from the organ pass through a coded aperture onto x-ray film. The image recorded on the film is a shadowgram (with properties similar to a hologram) and is a scrambled version of the organ; it must be decoded in order to view the reconstructed image. Reconstruction is accomplished by passing a laser beam through a photographically reduced copy (1:100) of the shadowgram. This simple procedure automatically unscrambles and displays the image on a screen. Different depths in the organ can be viewed by moving a lens in the laser system, thereby bringing one slice into focus while blurring overlying and underlying layers.

Received Dec. 27, 1976; revision accepted March 21, 1977.

For reprints contact: B. Leonard Holman, Dept. of Radiology, Harvard Medical School, 25 Shattuck St., Boston, MA 02115.

* Current address: Div. of Cardiovascular Radiology, The New York Hospital–Cornell Medical Center, 525 E. 68th St., New York, NY 10021.

The image at each depth is photographed to retain a permanent record.

The camera has no electronic parts, weighs 25 lb, and is held by a portable stand. With the front of the camera 5 cm from the organ of interest, the image area is 20 × 20 cm and the resolution was measured as 0.64 cm (full width at half maximum) with about the same resolution in depth perception. These values are close to the theoretical predictions (*8*) for the camera's design parameters as described in the next paragraph.

The camera consists of two coded apertures ("opaque" lead strips alternating with "transparent" aluminum ones) and a cassette for film to detect the photons passing through the two apertures (*8*). The first coded aperture, called a half-tone screen, is a set of equally spaced, parallel lead bars. The second coded aperture is a lead replica of an off-axis Fresnel zone plate, and is located midway between the half-tone screen and the film cassette. The detector consists of Kodak RP/R film in a standard x-ray cassette containing two Dupont Lightning-Plus screens. The cassette's size is 10 × 12 in. and it is about 10% efficient in detecting 140-keV radiation. The spacing of the lead rings in the zone plate varies across the 14-cm diam from 2.4 to 7.0 line pairs/cm. The lead thickness is 0.07 cm, which stops 75% of the photons incident on a ring. The spacing of the straight bars in the half-tone screen is 2.4 line pairs/cm, constant across the 14-cm diam. Separation between the half-tone screen and zone plate is 9 cm, and that between the zone plate and film cassette is 9 cm, giving a total camera length of 18 cm.

Nine mongrel dogs (weighing 15–22 kg) were anesthetized with phenobarbital (30 mg/kg). In six dogs, a catheter guidewire system (*9*) with a 3-mm plug was introduced into the femoral artery. The plug was made of occluded catheter material placed on the tip of the guidewire. Under fluoroscopic control, the left coronary ostium was selectively entered. After the system was positioned in the left main coronary artery, the guidewire was pulled back, releasing the 3-mm plug into the artery.

Ten minutes after embolization in the six occluded dogs, 100,000 microspheres (20–40 μ) labeled with 20 mCi of technetium-99m were injected into the left main coronary artery under fluoroscopic control. In two unoccluded dogs, 20 mCi of Tc-99m microspheres were similarly injected into the left coronary artery. In a third unoccluded dog, catheter streaming was intentionally induced, preferentially depositing microspheres into the distribution of the distal left anterior descending artery.

Imaging of the live dogs with the Fresnel-zone camera was performed immediately after injection. Images were obtained in the right and left anterior oblique positions (45°), and, when possible, in the right and left laterals. Five-minute exposures were obtained; thus the product of dose and exposure time was 200 mCi–minutes. Since the sensitivity of the Fresnel-zone camera is 5% of the Anger camera's, a comparable scintiscan containing 500,000 counts took 15 sec with the latter instrument. The low sensitivity of the Fresnel-zone camera is primarily due to the poor sensitivity of the detector.

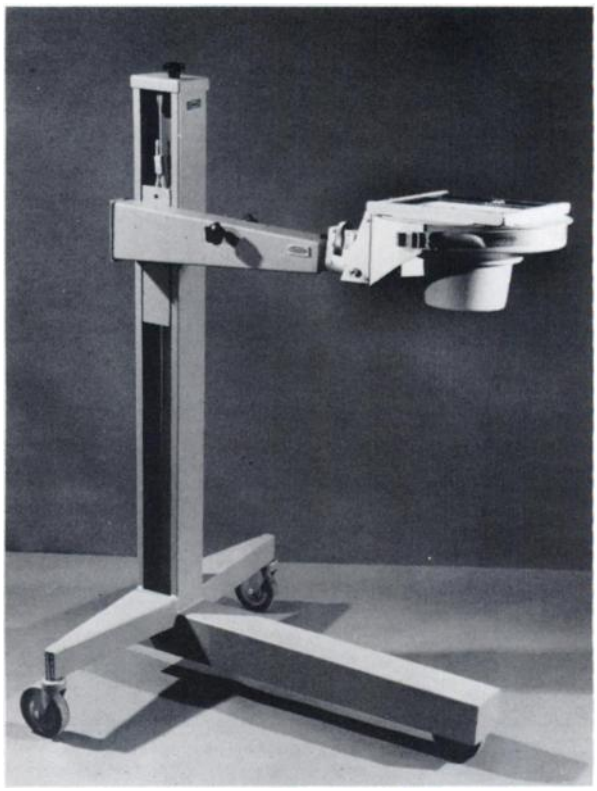

FIG. 1. The Fresnel-zone tomographic camera.

After completion of the Fresnel-zone imaging, the animals were killed and imaging was performed in the dead animal (to simulate a physiologically gated study) using an Anger-type scintillation camera with large-field-of-view camera and converging collimator. The animal was positioned in the right and left anterior oblique and right and left lateral positions, and 500,000 counts were collected for each projection.

After imaging, the left ventricular wall and septum were sectioned into 1- to 2-g specimens, and radioactivity in each specimen was assayed in a gamma well counter. The activity concentrations were recorded as percentages of the maximum concentration. The weight of tissue with a tracer concentration less than 30% of the maximum was de-

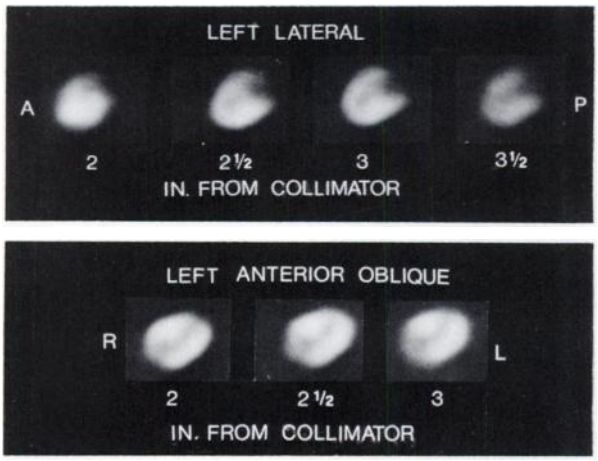

FIG. 2. Myocardial perfusion images in normal dog made with the instrument of Fig. 1: Top is left lateral; bottom is left anterior oblique.

termined and expressed as a percentage of the total weight of the left ventricle and septum.

The presence and extent of perfusion deficits was determined visually from the Fresnel-zone images by an observer without knowledge of the in vitro estimate of altered perfusion. Outlines of the left ventricular wall, ventricular cavity, and perfusion defect, were traced over the Fresnel-zone image, and for each projection the extent of perfusion defect was determined as a percentage of total ventricular area after subtracting the ventricular cavity. Measurements were performed for each tomographic image obtained between 2 and 4 in. (in 0.5-in. increments) from the collimator surface. The size of the perfusion defect (expressed as the percentage of altered left ventricular perfusion) was determined for each projection (right and left anterior oblique, right and left lateral) by averaging the percentage of altered perfusion for the five tomographic images obtained in that position. The extent of the perfusion deficit was then compared with the extent of perfusion reduction calculated from the in vitro assay of the tissue sections.

RESULTS

The reconstructed Fresnel-zone camera image in the two control dogs showed uniform distribution of the radiolabeled microspheres throughout the left ventricular wall and septum. Images obtained in multiple projections in the living closed-chested animal are shown in Fig. 2. In the left lateral projection (Fig. 2A), a relatively uniform distribution of the radiotracer is seen in the image focussed two inches from the collimator face, at the level of the lateral wall of the left ventricle. By 2.5 and particularly 3 in., the outline of the left ventricle comes into focus. The posterior papillary muscle is seen extending into the left ventricular cavity. In the left anterior oblique projection (Fig. 2B), the left ventricle is homogeneously perfused while the ventricular cavity has a dumbbell-shaped appearance due to the intrusion of the papillary muscles into the cavity. Both the anterior (above) and posterior (below) wall of the ventricle are well seen in this projection because the long axis of the ventricle is almost perpendicular to the collimator.

Perfusion defects were detected with the Fresnel-zone camera images in all four dogs with obstruction of the left anterior descending artery, and in two dogs with obstruction of the circumflex. Perfusion defects could be distinguished easily from the left ventricular cavity (Fig. 3). The perfusion defect is seen 2.0 in. from the collimator, before the left ventricular cavity comes into focus. Even when the cavity is clearly delineated (2.5 in.), the perfusion defect is seen as a separate structure.

Separation of subepicardial from subendocardial perfusion is seen in Fig. 3A. While the perfusion defect is transmural in the anterior wall, persisting subepicardial perfusion is seen at the apex despite diminished subendocardial perfusion. Thus the subendocardial region appears markedly underperfused but surrounded by a rim of well-perfused subepicardium.

In one unembolized animal, many microspheres were deposited in a small region of myocardium (6 g) perfused by the distal portion of the left

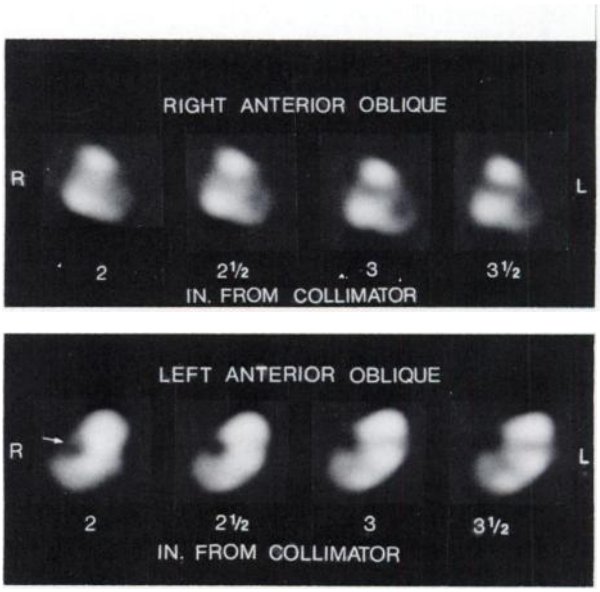

FIG. 3. Myocardial perfusion images following occlusion of the left anterior descending artery. Perfusion defect involves anterior wall and apex: top is right anterior oblique; bottom is left anterior oblique.

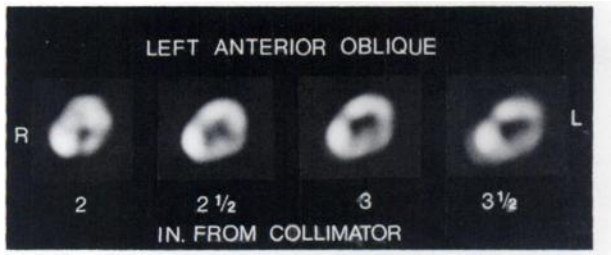

FIG. 4. Increased activity in region of septum after catheter streaming of Tc-99m microspheres.

anterior descending artery. The concentration of radioactivity was twice that of the remaining left ventricular cavity. Images obtained in this animal demonstrated the area of increased activity separated from the rest of the left ventricle by a thin band of decreased intensity (Fig. 4). This band surrounding the region of increased uptake is an artifact produced by the coded aperture reconstruction. An artifact of this type arises when there is a large, abrupt change in local activity and is not evident when the activity changes gradually. The artifact appears as a ring or band surrounding the hot spot. Because it occurs only with an abrupt activity gradient, we did not observe it in the experimentally embolized dogs.

Determination of the extent of the perfusion deficit from the Fresnel-zone camera images resulted in a mean absolute error of 18.4% in the left anterior oblique projection and 23.9% in the right anterior oblique projection. When the size of the perfusion defects seen on the left anterior oblique and right anterior oblique projections were averaged, the mean error was 13.6% (Table 1).

While perfusion defects were seen in Anger-camera images in all six animals with coronary occlusion, sizing of the defect was not possible because defects were not seen consistently in all views in the same dog, and because the perfusion defect could not be clearly separated from the left ventricular cavity. Furthermore, the perfusion defects were more sharply outlined on the Fresnel-zone images than on the Anger camera scintigrams, and separation of the ventricular cavity from the perfusion defect was more clearly defined with the tomographic Fresnel-zone images (Fig. 5).

DISCUSSION

Estimates of regional myocardial perfusion using radionuclide techniques have been limited by the constraints of the conventional two-dimensional imaging techniques available today (*10,11*). Superimposition of the anterior and posterior ventricular walls and separation of the ventricular cavity from regions of altered perfusion are two examples of the problems that arise.

Tomographic imaging techniques promise to overcome these handicaps. Three-dimensional image reconstruction using positron-emitting radiotracers has been applied to the myocardium, and with this technique myocardial perfusion has been estimated (*12*) and acute infarction has been detected (*13*). Unfortunately, three-dimensional reconstruction imaging with positron-emitting tracers is an expensive and cumbersome method, available to only a few medical centers. Furthermore, resolution is poor with currently available instruments.

Our study showed that accurate tomographic images of regional myocardial perfusion can be obtained using gamma-emitting tracers, a readily portable, inexpensive scintillation camera, and a

TABLE 1. SCINTIGRAPHIC MEASUREMENT OF THE EXTENT OF ALTERED MYOCARDIAL PERFUSION

Dog No.	Lesion	Size of perfusion defect				Percent error†		
		In vitro assay*	LAO**	RAO**	LAO and RAO‡	LAO	RAO	LAO and RAO
1	LAD	8.0	7.0	14.2	9.0	−12.5	+77.5	+12.5
2	LAD	13.0	12.2	14.6	13.4	−6.1	+8.8	+3.1
3	LAD	17.3	22.8	17.7	20.3	+31.8	+2.3	+17.3
4	LAD	14.4	10.1	7.6	8.9	−29.9	−47.2	−38.2
5	CFX	9.5	7.4	9.6	8.5	−22.1	+1.1	−10.5
6	CFX	10.4	11.2	9.7	10.4	+7.7	−6.7	0
		12.1	11.8	12.2	11.8	|18.4|	|23.9|	|13.6|

* As percent of total ventricular weight.

** As percent of ventricular area.

† $\frac{\text{size of perfusion defect from image} - \text{size by assay}}{\text{size of perfusion defect by in vitro assay}}$

‡ $\frac{\text{size of perfusion defect in LAO projection} + \text{size of defect in RAO}}{2}$

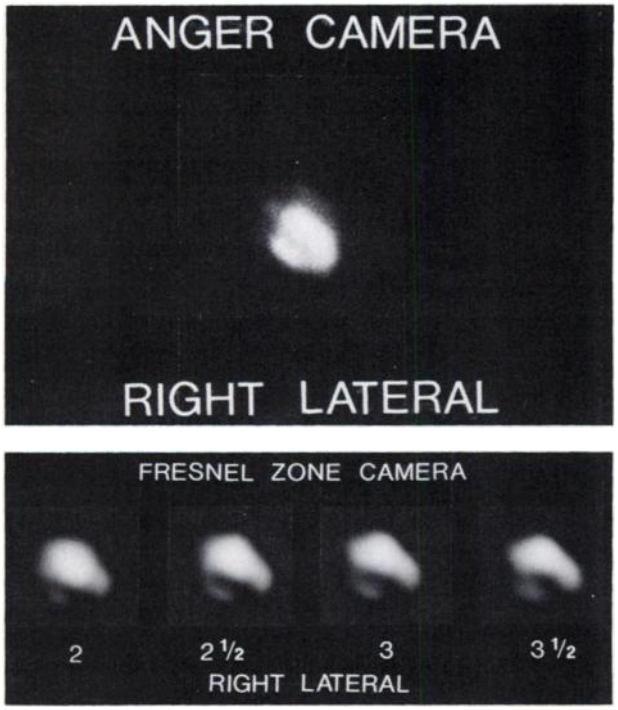

FIG. 5. Myocardial perfusion scintigraphy with Anger camera (top), and Fresnel zone-plate camera (bottom), after occlusion of left circumflex artery (right lateral view). Perfusion defect along inferior wall is more clearly defined on Fresnel-zone image.

Fresnel-zone collimator. The size of the perfusion defect can be estimated accurately and can be separated from other anatomic structures after a coronary artery injection of the radiotracer. Sizing is most accurate for regions of markedly reduced flow (<30% of normal). In man, the technique would therefore appear best suited for the determination of the extent of scar tissue, and might be useful in predicting the extent of nonviable myocardium.

Myocardial perfusion imaging after the coronary artery injection of Tc-99m microspheres is ideally suited to the Fresnel-zone camera because the target organ is small and the target-to-background ratio is high. When this ratio is low (for example, if the tracer were distributed to surrounding tissue as well as the target organ), signal artifacts due to superimposed and adjacent structures become an increasing problem. In addition, direct injection places a large fraction of the dose within the target organ and compensates for the poor sensitivity of the camera system.

The major limitation of the Fresnel-zone camera is its poor sensitivity (*8,14*). The dose-exposure time of 200 mCi–min required for optimal imaging would result in long imaging times in man when relatively small doses of the radiotracer are injected. With 10 mCi of Tc-99m microspheres, 20-min exposures would be required. Three solutions to this problem are feasible. First of all, faster film screens could be constructed, specifically designed for the 140-keV energy range. Secondly, a different detector could be used with the Fresnel-zone collimator. The Anger camera can be used as a detector, but it cannot handle the high photon flux that reaches the detector because of the high transmittance of the Fresnel-zone collimator (*15*). The multiwire proportional chamber may be a suitable detector because of its high data-rate capacity (*16*). Finally, a radionuclide with a lower energy and shorter half-life than those of technetium-99m could be used as the microsphere label. Tantalum-178 ($T_{1/2} = 9.4$ min) would be one such candidate (*17*).

The use of a Fresnel-zone camera to determine the extent of perfusion abnormalities is a promising prototype method to estimate the extent of myocardial fibrosis. This method will complement the coronary arteriogram and other techniques that provide quantitative estimates of the degree of flow reduction (*18,19*) and the adequacy of coronary reserve (*20*).

ACKNOWLEDGMENT

This work was supported in part by USPHS Grants GM 18674 and HL 17739 and by American Heart Association Grant 75 796.

REFERENCES

1. ZARET BL, STRAUSS HW, MARTIN ND, et al.: Noninvasive regional myocardial perfusion with radioactive potassium. Study of patients at rest, with exercise and during angina pectoris. *N Engl J Med* 288: 809–812, 1973

2. ROMHILT DW, ADOLPH RJ, SODD VC, et al.: Cesium-129 myocardial scintigraphy to detect myocardial infarction. *Circulation* 48: 1242–1251, 1973

3. MARTIN ND, ZARET BL, MCGOWAN RL, et al.: Rubidium-81: a new myocardial scanning agent. *Radiology* 111: 651–656, 1974

4. LEBOWITZ E, GREENE MW, BRADLEY-MOORE P, et al.: ^{201}Tl for medical use. *J Nucl Med* 14: 421–422, 1973

5. HOLMAN BL, ELDH P, ADAMS DF, et al.: Evaluation of myocardial perfusion after intracoronary injection of radiopotassium. *J Nucl Med* 14: 274–278, 1973

6. JANSEN C, JUDKINS MP, GRAMES GM, et al.: Myocardial perfusion color scintigraphy with MAA. *Radiology* 109: 369–380, 1973

7. RITCHIE JL, HAMILTON GW, GOULD KL, et al.: Myocardial imaging with indium-113m- and technetium-99m-macroaggregated albumin. New procedure for identification of stress-induced regional ischemia. *Am J Cardiol* 35: 380–389, 1975

8. BARRETT HH, HORRIGAN FA: Fresnel zone plate imaging of gamma rays; theory. *Appl Optics* 12: 2686–2702, 1973

9. HOLMAN BL, DEWANJEE MK, IDOINE J, et al.: Detection and localization of experimental myocardial infarction with ^{99m}Tc-tetracycline. *J Nucl Med* 14: 595–599, 1973

10. HOLMAN BL: Radionuclide methods in the evaluation of myocardial ischemia and infarction. *Circulation* 53: Suppl 1, 112–119, 1976

11. TER-POGOSSIAN MM: Limitations of present radionuclide methods in the evaluation of myocardial ischemia and infarction. *Circulation* 53: Suppl 1, 119–121, 1976

12. WEISS ES, HOFFMAN EJ, PHELPS ME, et al.: External detection and visualization of myocardial ischemia with ^{11}C-substrates in vitro and in vivo. *Circ Res* 39: 24–32, 1976

13. ADAMS DF, HESSEL SJ, JUDY PF, et al.: Computed tomography of the normal and infarcted myocardium. *Am J Roentgenol* 126: 786–791, 1976

14. FARMELANT MH, DEMEESTER G, WILSON D, et al.: Initial clinical experiences with a Fresnel zone-plate imager. *J Nucl Med* 16: 183–187, 1975

15. BUDINGER TF, MACDONALD B: Reconstruction of the Fresnel-coded gamma camera images by digital computer. *J Nucl Med* 16: 309–313, 1975

16. PEREZ-MENDEZ V, KAUFMAN L, LIM CB, et al.: Multiwire proportional chambers in nuclear medicine: present status and perspectives. *Int J Nucl Med Biol* 3: 29–33, 1976

17. HOLMAN BL, JONES AG, HARRIS GI, et al.: ^{178}Ta—a new short-lived radionuclide for low energy gamma cameras: production and separation (abstract). *J Nucl Med* (in press)

18. CANNON PJ, DELL RB, DWYER EM: Regional myocardial perfusion rates in patients with coronary artery disease. *J Clin Invest* 51: 978–994, 1972

19. HOLMAN BL, ADAMS DF, JEWITT D, et al.: Measuring regional myocardial blood flow with ^{133}Xe and the Anger camera. *Radiology* 112: 99–107, 1974

20. HOLMAN BL, COHN PF, ADAMS DF, et al.: Regional myocardial blood flow during hyperemia induced by contrast agent in patients with coronary artery disease. *Am J Cardiol* 38: 416–421, 1976